研究简报

Co-Fe 普鲁士蓝类配合物纳米颗粒的微乳液法制备与表征

方　建[1]　杜贤龙[1]　吕辉鸿[1]　郭　丹[1]　赵继华[*,1]　沈伟国[2]

([1] 兰州大学化学化工学院,兰州　730000)
([2] 华东理工大学化学学院,上海　200237)

Synthesis and Characterization of Cobalt-iron Prussian Blue Analogue Nanoparticles by Microemulsion

FANG Jian[1]　DU Xian-Long[1]　LU Hui-Hong[1]　GUO Dan[1]　ZHAO Ji-Hua[*,1]　SHEN Wei-Guo[2]
([1]Department of Chemistry, Lanzhou University, Lanzhou 730000)
([2]Department of Chemistry, East China University of Science and Technology, Shanghai 200237)

Abstract: Highly oriented cubic, hollow cubic and spherical nanoparticles of cobalt-iron Prussian blue analogues were synthesized in poly oxyethylene tertoctylphenyl ether (TritonX-100)/n-hexanol/cyclohexane microemulsion. The effects of the water-to-surfactant molar ratio (w), the reactant concentration and the reaction temperature on the morphology of cobalt-iron Prussian blue analogues were studied. The samples were characterized by transmission electron microscopy (TEM), field emission scan electron microscopy (FE-SEM), energy-dispersive X-ray spectroscopy (EDS), X-ray diffraction (XRD) and infrared spectroscopy (IR).

Key words: microemulsion; Triton X-100; Prussian blue analogues; nanoparticle

Transition metal hexacyanoferrates of the general formula $A_h M_k[N(CN)_6]_l \cdot x H_2O$ (h, k, l, x=stoichiometric numbers, A=alkali metal cation, M and N=transition metal ions; and M ion is high-spin (HS), N ion is low-spin(LS)) present an important class of mixed-valence compounds, namely Prussian blue analogues (PBA). The structure of the PBA is highly symmetrical, most often a face-centered cubic lattice (unit cell length: about 102 nm) with octahedral coordination of the M and N ions by $N \equiv C$ and $C \equiv N$ ligands, respectively[1]. The alkali metal cations, A, which provide charge compensation, are located in the tetrahedral sites[2]. If no alkali metal cations are in these structures, water

molecules will locate in these sites. In this case, the inherent structures are loose and the crystallization will be difficult[3]. These compounds have aroused intense recent interest because of their electrocatalytic, electrochromic, ion-exchange, ion-sensing and photomagnetic properties[1]. Especially in the field of molecular magnets, the PBA have been extensively investigated. Hashimoto and co-workers reported that the cobalt-iron cyanide ($K_{0.2}Co_{1.4}[Fe(CN)_6]_6 \cdot 9H_2O$) not only had the general magnetization of PBA but also the photoinduced magnetization at low temperature in 1996[4]. Such photocontrol over the magnetic properties is important from the viewpoint of practical applications

as well as the basic science. Photo-tunable magnets can be used in future memory devices, optical switches and so on[5].

Although much work has focused on the relationship between the unit cell structure and magnetic properties, relatively few attempts have been made to control the size, shape and higher-order organization of these materials. In fact, the magnetic properties are very sensitive to the morphology of materials due to the dominating role of anisotropy in magnetism. Different shape and size of the molecular magnets can result in the change of magnetic properties[6-10]. Gao′s group reveals that the PBA exhibit interesting magnetic behavior, especially for their coercivities, which are dependent on the effect of shape anisotropy [7]. But the preparation of cobalt-iron PBA nanomaterials using the method of microemulsion "soft template" was very limited and the morphology of particles was single and unchangeable[8,11].

In this note, the synthesis of cobalt-iron PBA nanoparticles is reported with various morphologies (cube, hollow cube, sphere) in nonionic surfactant Triton X-100 microemulsion system. To the best of our knowledge hollow cubic cobalt-iron PBA nanocrystals have not yet been reported.

1　Experimental

1.1　Materials

The nonionic surfactant Triton X-100 (poly oxyethylene tertoctylphenyl ether, C.P.) and n-hexanol (C.P.) were purchased from Fluka, and cyclohexane (A.R.) from Tianjin Chemical Reagent Limited Company. Cobalt chloride hexahydrate (CoCl2·6H2O, A.R.) and potassium ferricyanide (K3Fe(CN)6, A.R.) were purchased from Tianjin Guangfu Fine Reagent Factory. Double distilled water was used thoughout.

1.2　Preparation

The surfactant (TritonX-100), cosurfactant (n-hexanol) and oil phase (cyclohexane) were mixed with a weight ratio of 2∶1∶1 by magnetically stirring until formation of a transparent mixture emulsion (ME). In a typical synthesis, 5 g of 6 mmol·L^{-1} CoCl2 aqueous solution was added to 10 g ME to form microemulsion

M(I), and microemulsion M(II) was formed through adding 5 g of 6 mmol·L^{-1} K3Fe(CN)6 aqueous solution to 10 g ME. M(I) was added dropwise to the M(II) under magnetically stirring. Then the two microemulsions were mixed and magnetically stirred for 4.5 hours at 28.5 ℃. At last, the mixed microemulsions were heated and centrifuged at 12 000 r·min^{-1} for about 10 min. The precipitate was then thoroughly washed in a 1∶1 (V/V) mixture of ethanol and H2O for 5 times to remove the contaminated oil, surfactant and other inorganic substance from the particles.

1.3　Characterization

XRD patterns were collected on a Rigaku D/MAX-2400 X-ray diffractometer with graphite monochromatized Cu $K\alpha$ radiation (λ=0.154 06 nm). Hitachi H-600 transmission electron microscopy (TEM) and Hitachi S-4800 field emission scan electron microscopy (FE-SEM) were taken to examine the morphology and dimension of the cobalt-iron PBA nanoparticles. Elemental analyses of the products were conducted by the KEVEX energy-dispersive X-ray spectroscopy (EDS). The FTIR spectrum was recorded with NEXUS670 IR spectrometer. The diameter of the reverse micelles was measured by BI-200SM (Brookhaven) dynamic light-scattering (DLS).

2　Results and discussion

2.1　XRD analysis

The structure and chemical composition of cobalt-iron PBA samples synthesized in w=45, c_{CoCl_2}=$c_{K_3Fe(CN)_6}$ =6 mmol·L^{-1}, T=28.5 ℃ were confirmed with XRD and the typical pattern was shown in Fig.1. We
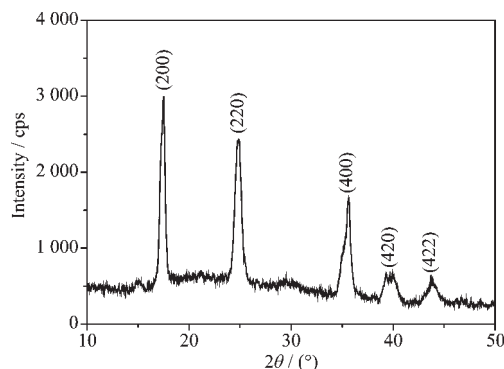
Fig.1　XRD pattern of cobalt-iron PBA samples synthesized in w=45, c_{CoCl_2}=$c_{K_3Fe(CN)_6}$=6 mmol·L^{-1}, T=28.5 ℃

observe sharp intense peaks at 2θ values, 17.20°, 24.48°, 34.86°, 39.12°, 43.62°, corresponding to the {200}, {220}, {400}, {420} and {422} reflections. Yakhmi et al.[12] reported the XRD pattern of cobalt-iron PBA with face-centered cubic structure and calculated the unit cell lattice parameter (a=103 nm). Our results are consistent with their report.

2.2 EDS and IR analysis

Prussian blue analogues are known to exist in a so-called "solube" form, potassium-rich, and an insoluble modification, potassium-free. In the case of cobalt-iron PBA, the soluble form has the composition of $KCo[Fe(CN)_6]$ and the stoichiometric formulas of the potassium-free salts is $Co_3[Fe(CN)]_2$. It may be noted that the term "solube" only refers to the colloid solubility and not to an ionic solubility of the complex salt[13]. To find out the form of the products, the elemental composition of the cobalt-iron PBA was determined using EDS measurements. Typical EDS spectrum of cobalt-iron PBA is shown in Fig.2. The cobalt-iron PBA exhibits three strong $K\alpha$ peaks for Co (6.95 keV), Fe (6.40 keV) and K (3.31 keV). The quantitative evaluation of the peak areas allows an estimation of the molar ratios of K, Co, Fe (0.6 : 1.32 : 1). It can be recognized that the cobalt-iron PBA consist of the soluble modification, potassium-containing, and the formula may be $K_{0.6}Co_{1.32}[Fe(CN)_6]$. The infrared (IR) spectrum measurement at room tempera-ture in the region from 2 000 to 2 200 cm^{-1} showed two peaks at 2 159.8 cm^{-1} (Fe^{III}-CN-Co^{II}) and 2 092.79 cm^{-1} (Fe^{II}-CN-Co^{II}).
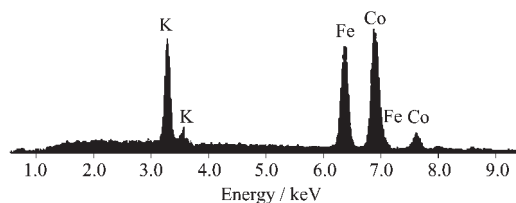
Fig.2　EDS spectrum of cobalt-iron PBA synthesized in w=45, c_{CoCl_2}=$c_{K_3Fe(CN)_6}$=6 mmol·L^{-1}, T=28.5 ℃

2.3 Morphology control

2.3.1 Effect of water-to-surfactant molar ratio (w)

The water-to-surfactant molar ratio (w) is an important parameter for the determination of the hydrodynamic radius of the water droplets. Fig.3 shows TEM images of the samples prepared from microemulsion with different w (15 to 50) and other conditions fixed to c_{CoCl_2}=$c_{K_3Fe(CN)_6}$=6 mmol·L^{-1}, T=28.5 ℃. As the w was 15, the diameter of products was very small (ca. 15 nm), but the aggregation of spherical particles was serious (TEM image was not shown). From the Fig.3a, it can be seen that only spherical nanoparticles with the diameter of about 30 nm are obtained when the w is 25. With the increasing of w, the "water pool" becomes larger and the rigidity of the Triton X-100-water interface is reduced, cobalt-iron PBA nanoparticles are easy to grow to the morphology of cube.
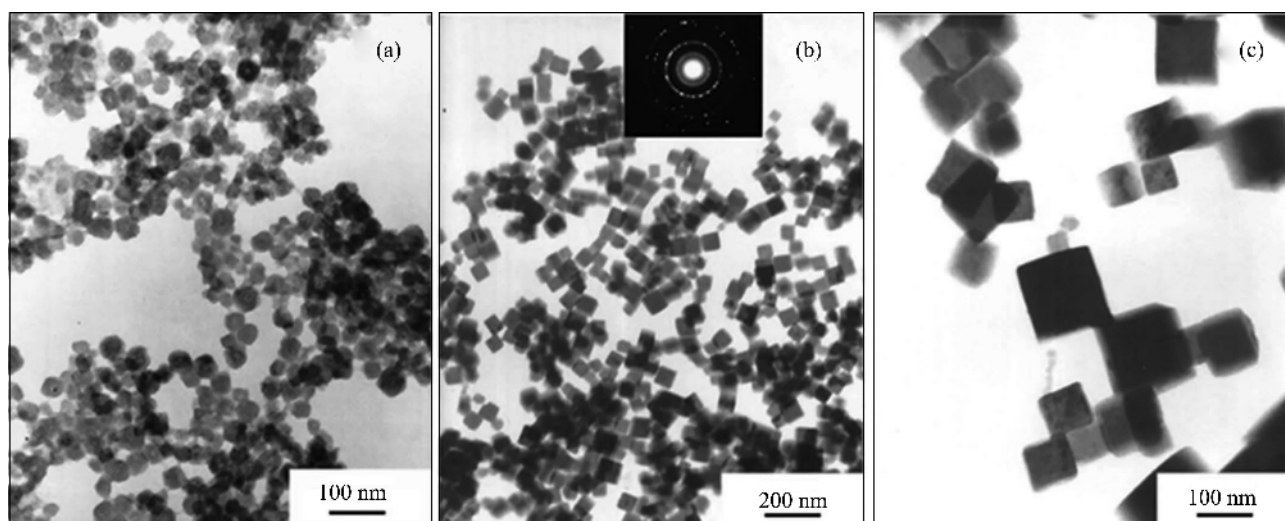
(a) w=25, (b) w=45, (c) w=50

Fig.3　TEM images of cobalt-iron PBA prepared at different w (c_{CoCl_2}=$c_{K_3Fe(CN)_6}$=6 mmol·L^{-1}, T=28.5 ℃)

When the w is 45, cobalt-iron PBA cubic nanoparticles with the dimension of 60 nm are obtained (Fig. 3b). The inset in Fig.3b is the electron diffraction pattern of the cubic nanoparticles with a dimension of 60 nm. When the w is up to 50, the rigidity of the Triton X-100-water interface is so poor that the aggregation of the particles becomes serious, the cubic nanoparticles are no longer uniform and the dimensions are between 50 to 140 nm (Fig.3c).

In each case, however, the nanoparticles are significantly larger than those predicted on the basis of a statistical distribution of reactants between the nanometer-sized water droplets. For example, the hydrodynamic radius is about 10.8 nm from dynamic light-scattering (DLS) as w is 45, but the cubic nanoparticles are obtained with the dimension of 60 nm. In fact, at 6 mmol·L^{-1} and w=45, there were approximately 19 ions in each water filled cage. A 60 nm cubic nanoparticle contains approximately 210 000 unit cells, $i.e.$ 840 000 $[Fe(CN)_6]^{3-}$ and 840 000 Co^{2+} ions. This means that about 45 000 droplets would be the place to produce one crystal of the size observed[11]. There are about 1.4×10^{18} droplets in w=45, c_{CoCl_2}= $c_{K_3Fe(CN)_6}$=6 mmol·L^{-1}, T=28.5 ℃, but only 3.7×10^{15} droplets would be filled with cobalt-iron PBA nanoparticles. From above analysis, we could clearly conclude that most of the droplets are empty after the reaction.

2.3.2　Effect of reactant concentration

Fig.4 lists the images of cobalt-iron PBA nanoparticles with various reactant concentrations and other conditions fixed in w=45, c_{CoCl_2}=$c_{K_3Fe(CN)_6}$=6 mmol·L^{-1}, T=28.5 ℃. When the concentration of reactants is all 2 mmol·L^{-1} or 4 mmol·L^{-1}, the average dimension of cobalt-iron PBA cubic nanoparticles is about 110 nm (Fig.4a). When 6 mmol·L^{-1} $CoCl_2$ and 6 mmol·L^{-1} $K_3Fe(CN)_6$ were used, $i.e.$ the typical condition, the size was about 60 nm and very uniform (Fig.3b). The inverse relationship between size and concentration is consistent with a nucleation-controlled process, in which the number of nucleus rises as the supersaturation (concentration) is increased, as the consequence

the average particle size is diminished. However, when the concentration of reactants is all 9 mmol·L^{-1} or 12 mmol·L^{-1}, the hollow cubic cobalt-iron PBA nanocrystals with size about 30 nm are obtained (Fig. 4b). The broken hollow shells (Fig.4c) obviously reveal the hollow structure. Usually, the surface energies associated with different crystallographic planes are different, and a general sequence may hold: $\gamma\{111\} < \gamma\{100\} < \gamma\{110\}$[14]. As illustrated by Wang[14], the shape of a fcc nanocrystal was mainly determined by the ratio R between the growth rates along the <100> and <111> directions. Perfect cubes bound by the less stable {100} planes could be achieved if R is reduced to 0.58. For the nanocubes with the slight holes illustrated in Fig.4c, the ratio R should have a value lower than 0.58[15].
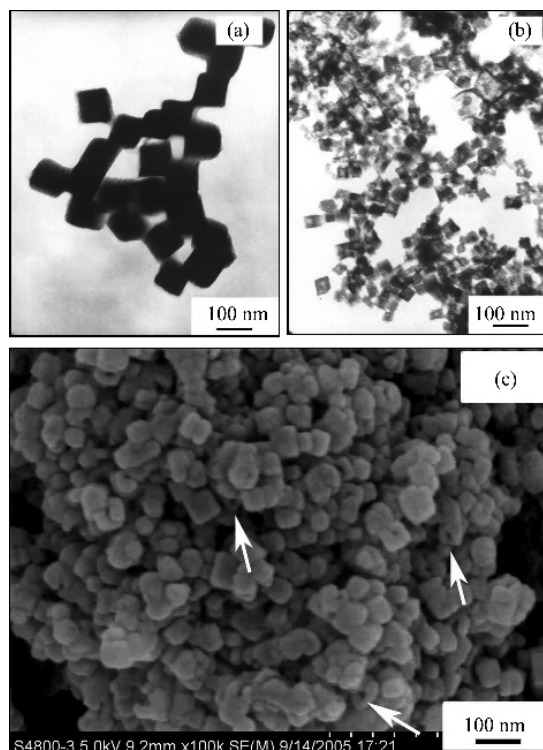
(a) c_{CoCl_2}=$c_{K_3Fe(CN)_6}$=2 mmol·L^{-1} /4 mmol·L^{-1}, (b) c_{CoCl_2}=$c_{K_3Fe(CN)_6}$=9 mmol·L^{-1}, (c) FE-SEM of Co-Fe PBA prepared at c_{CoCl_2}=$c_{K_3Fe(CN)_6}$=9 mmol·L^{-1}

Fig.4　TEM images of cobalt-iron PBA prepared at different concentration of reactants (w=45, T=28.5 ℃)

2.3.3　Effect of reaction temperature

From Fig.5 we can see the obvious effect of reaction temperature. The cubic nanoparticles are

obtained with a mean size of 50 nm at 24.5 ℃ (Fig. 5a). When the reaction temperature is increased to 28.5 ℃, the uniform cubic nanoparticles are achieved with an average dimension of 60 nm (Fig.3c). But when the reaction temperatures are reached at 31.5 ℃, the products with a mean size of 40~100 nm are obtained (Fig.5b). In fact, the microemulsion will be no longer stable when the temperature is too low or too high. So the products obtained from the microemulsion tend to aggregation and the cubic nanoparticles become no longer uniform (Fig.5a and Fig.5b).
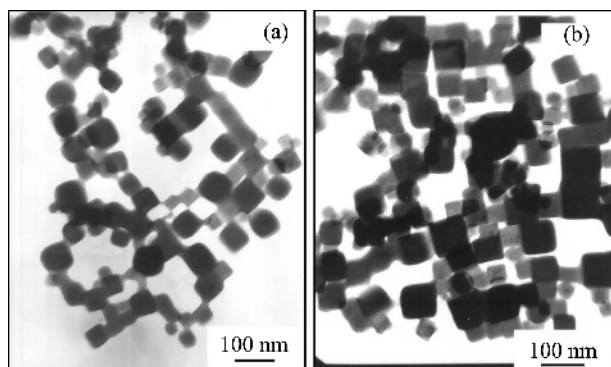

Fig.5   TEM images of cobalt-iron PBA prepared at different reaction temperatures (w=45, c_{CoCl_2}= $c_{K_3Fe(CN)_6}$=6 mmol·L^{-1})

3   Conclusions

Highly oriented cubic, hollow cubic and spherical nanoparticles of cobalt-iron PBA nanoparticles were prepared in the reverse microemulsion system formed by nonionic surfactant Triton X-100. The size and morphology of the products can be controlled by changing the value of w, reactant concentration and reaction temperatures.

Referances:

[1] Tacconi N R, Rajeshwar K. *Chem. Mater.*, **2003,15**:3046~ 3062

[2] Mallash T, Thiebaut S, Verdaguer M, et al. *Science*, **1993, 262**:1554~1557

[3] Buser H J, Schwarzenbach D, Petter W, et al. *Inorg. Chem.*, **1977,16**:2704~2710

[4] Sato O, Iyoda T, Fujishima A, et al. *Science*, **1996,272**:704~ 705

[5] Sato O. *J. Photochem. Photobiol. C, Chem. Rev.*, **2004,5**:203 ~223

[6] Uemura T, Kitagawa S. *J. Am. Chem. Soc.*, **2003,125**:7814~ 7815

[7] SUN Hao-Ling, SHI Hong-Tao, GAO Song, et al. *Chem. Commun.*, **2005**:4339~4341

[8] Chow P Y, Ding J, Wang X Z, et al. *Phys. Stal. Sol. (a)*, **2000, 180**:547~553

[9] ZHOU Ping-Heng, XUE De-Sheng, CHEN Xing-Guo, et al. *Nano Lett.*, **2002,2**:845~847

[10]Catala L, Gacoin T, Mallah T, et al. *Adv. Mater.*, **2003,15**: 826~829

[11]Vaucher S, Fielden J, Li M, Mann S, et al. *Nano Lett.*, **2002, 2**:225~229

[12]Choudhury S, Dey G K, Yakhmi J V. *J. Crystal Growth*, **2003, 258**:197~203

[13]JIN Wang-Qin, Pyrasch M, Tieke B, et al. *J. Phys. Chem. B*, **2003,107**:12062~12070

[14]WANG Zhong-Lin. *J. Phys. Chem. B*, **2000,104**:1153~1175

[15]ZHOU Guang-Jun, LU Meng-Kai, YANG Zhong-Sen. *Langmuir*, **2006,22**:5900~5903